# Red to Near-Infrared Isoindole BODIPY Fluorophores: Synthesis, Crystal Structures, and Spectroscopic and Electrochemical Properties

Changjiang Yu, Qinghua Wu, Jun Wang, Yun Wei, Erhong Hao,* and Lijuan Jiao*

The Key Laboratory of Functional Molecular Solids, Ministry of Education, Anhui Laboratory of Molecule-Based Materials, School of Chemistry and Materials Science, Anhui Normal University, Wuhu 241000, China

S *Supporting Information*

ABSTRACT: A series of high-performance fluorophores named isoindole boron dipyrromethenes (BODIPYs) containing either symmetrical or unsymmetrical alkyl substitution patterns on pyrrole rings were synthesized by an efficient process and were characterized by X-ray diffraction and spectroscopic and electrochemical analyses. Most of these dyes show strong, sharp absorption and bright fluorescence emission in the red to near-infrared (NIR) region (up to 805 nm in acetonitrile). Pyrrolic alkyl substitutions lead to increases in the HOMO and LUMO energy levels and an overall decrease in the energy band gaps of the dye. Among the 23 isoindole BODIPY dyes synthesized, solvent-dependent fluorescence emission and lifetime decay were only observed for those containing a 3-methyl substituent on the uncoordinated pyrrole ring, whereas little variation in the fluorescence intensity was observed for the rest of the dyes upon changing the polarity of the solvent. These resultant dyes can be further functionalized via the Knoevenagel condensation on the α-methyl substituent of the chromophore to install a variety of functionalities, including a dimethylamine group demonstrated in this work. This dimethylamine-functionalized isoindole BODIPY shows weak fluorescence at 805 nm in acetonitrile and a ratiometric "turn-on" NIR fluorescence response to decreasing pH.
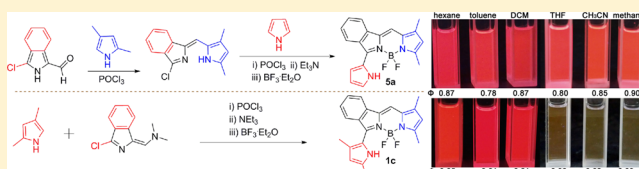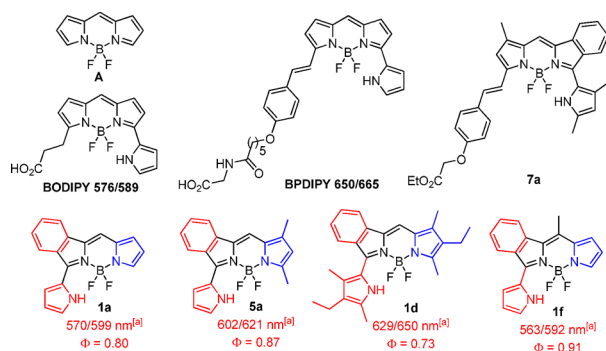
■ INTRODUCTION

Bright fluorescent dyes, especially those emitting in the red to near-infrared (NIR) region, are valuable for applications in biological systems.[1] Great efforts have been devoted to the fine-tuning of the photophysical and photochemical properties of many chromophores to achieve novel types of far-red to NIR organic fluorophores.[2] Boron dipyrromethenes (BODIPYs, Figure 1) have received increasing research interest in the past three decades because of their excellent optical properties and easy accessibility[3,4] and have been widely applied as laser dyes,[5] fluorescence labeling agents,[6] sensors,[7] fluorescent switches,[8]

Figure 1. Structure of BODIPY core (**A**), commercialized BODIPYs 576/589 and 650/665 marketed by Invitrogen, and isoindole BODIPYs **1a**, **5a**, **1d**, **1f**, and **7a** previously communicated by us. [a]Spectroscopic data were recorded in dichloromethane.

photovoltaics/optoelectronics,[9] and photosensitizers[10] in a varity of fields.

Classical BODIPYs generally absorb/emit at around 500 nm.[4] Besides fusing aromatic moieties onto the pyrrolic position of the chromophore,[11−13] extending the conjugation at the 3,5-positions[13−17] is a common way to achieve long wavelength NIR BODIPYs as already demonstrated by the two commercialized long wavelength BODIPYs (576/589 and 650/665, Figure 1).[18] However, the synthesis of these 3-pyrrole-substituted BODIPYs, although elegant, generally requires lengthy synthetic steps, the preparation of highly reactive intermediates, or the use of expensive metal catalysts.[19] Recently, we have communicated a one-pot synthesis of eight isoindole BODIPYs with symmetrical substitution patterns of pyrrole rings in good to excellent yields based on a POCl₃-promoted condensation of 3-chloro-1-formylisoindole **3** with suitable pyrroles (or indoles) (Scheme 1, route a).[20] These isoindole BODIPYs show strong absorption and emission bands centered at 570−650 nm, which can be further tuned to the NIR region via classic Knoevenagel condensation. Alberto and Simone performed theoretical calculations on the spin−orbit matrix elements between singlet and triplet excited state wave functions for these isoindole BODIPYs.[21] We have found that alkyl substitutions at both the pyrrole rings and the *meso*-position can greatly affect the absorption and emission bands of these isoindole BODIPYs in dichloromethane with a red-shift for pyrrolic substitution(s) and
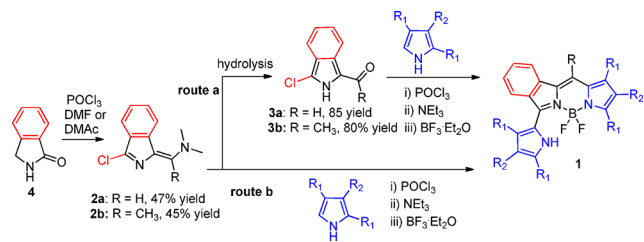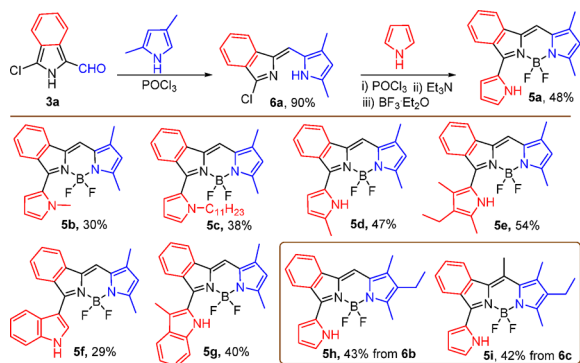
Scheme 1. Synthetic Routes for Isoindole BODIPYs 1a−h with Symmetrical Substitution Patterns of Pyrrole Rings: Route a, Our Previously Communicated Method; Route b, New Synthetic Route Presented in This Work


a blue-shift for *meso*-substitution (Figure 1). Interestingly, isoindole BODIPY **5a**, with an unsymmetrical alkyl substitution pattern of the pyrrole ring, gives not only a red-shift of the spectra but also an enhanced fluorescence quantum yield with respect to **1a** (Figure 1). These interesting preliminary spectroscopic results prompted us to further synthesize a set of isoindole BODIPYs **5** with unsymmetrical alkyl substitution patterns of pyrrole rings (Scheme 2) and perform detailed comparative

Scheme 2. Synthesis and Yields of Isoindole BODIPYs 5a−i with Unsymmetrical Substitution Patterns of Pyrrole Rings

studies on their X-ray diffraction and spectroscopic and electro-chemical properties with isoindole BODIPYs **1** possessing symmetrical substitution patterns of pyrrole rings (Figure 2).
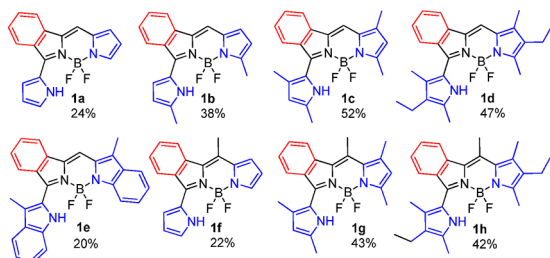
We also report a new synthetic route to BODIPYs **1** from the direct condensation of 3-chloro-isoindolylidene-*N*,*N*-dimethyl(m)ethanamine with suitable pyrroles or indoles (Scheme 1, route b).

■ RESULTS AND DISCUSSIONS

Synthesis. In our previous communication,[20] isoindole BODIPYs **1** with symmetrical substitution patterns of pyrrole

rings were obtained via the condensation of 3-chloro-1-formylisoindole **3a** with an excess amount of suitable pyrrole derivatives (Scheme 1, route a). In this work, we demonstrate that the step to hydrolyze **2** to generate **3a** can be skipped by directly applying **2** for the condensation reaction (Scheme 1, route b). This condensation requires comparatively higher temperature (80 °C in 1,2-dichloroethane) from which the desired isoindole BODIPYs **1a−h** (Figure 2) are isolated with comparable (20−52%) yields to those in our previous report.[20] However, at room temperature, it mainly generates the BF₂ complexes of dipyrromethenes. It is noteworthy that electron-deficient pyrroles and indoles give comparatively low yields (20−24% for **1a**, **1e** and **1f**) in comparison to those of alkyl-substituted pyrroles (38−52% for **1b−d** and **1g,h**) for this reaction.

To study the scope of this reaction and structure−property relationship of these isoindole BODIPYs, we synthesized **5a−i** with unsymmetrical substitution patterns of pyrrole rings according to Scheme 2. Key α-chlorodipyrromethenes **6a−c** were generated in 79−90% yields from the condensation of **3** with alkyl-substituted pyrrole in the presence of POCl₃. Subsequent nucleophilic substitution of α-chlorodipyrrome-thenes **6** smoothly proceeded with excess amounts of pyrrole and indole derivatives and gave isoindole BODIPYs **5a−i** in 29−54% isolated yields. However, the reaction time varies from 10 min to 12 h depending on the electronic properties of the nucleophile. For example, this reaction is accomplished within 10 min in the case of electron-rich 2,4-dimethyl-3-ethylpyrrole, whereas it requires 6−12 h when *N*-alkyl-substituted or unsubstituted pyrrole or indole was used. In contrast, highly electron-deficient 2-nitropyrrole did not react at all in this reacton.

These resulting isoindole BODIPYs can easily be further functionalized via the Knoevenagel condensation to install a variety of functionalities, for example, carboxylic ester groups (Figure 3), which upon hydrolysis can be used as a tethering


Figure 2. Yields for isoindole BODIPYs **1a−h** using route b in Scheme 1.
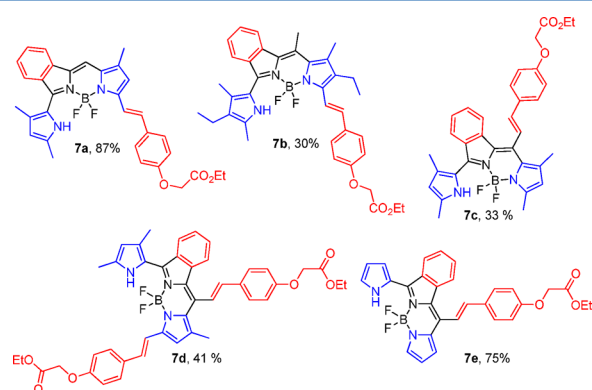
**Figure 3.** Structures and yields of isoindole BODIPYs **7a−e**.

group for bioimaging and labeling. Considering that a dimethylamino group is a fragment frequently used to tune the photophysical properties of chromophores via either an intra-molecular charge transfer (ICT) or a photoinduced electron transfer (PET) process,[22] we further applied **1d** for the Knoevenegal condensation with 4-(dimethylamino)benzaldehyde **8** to generate **7f** in 75% yield (Scheme 3), which shows weak fluorescence at 805 nm in acetonitrile and a ratiometric "turn-on" NIR fluorescence upon decreasing the pH.

X-ray Crystal Structure Analysis. Single crystals suitable for X-ray analysis for isoindole BODIPYs **1a**, **1b**, **1h**, **5b**, **5d−g**,

Scheme 3. Synthesis and Yield of Isoindole BODIPY 7f from Knoevenagel Reaction of Isoindole BODIPY 1d
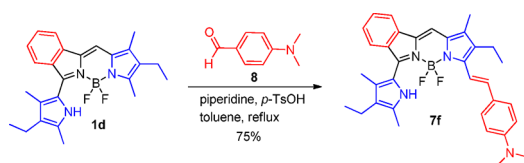
and **5i** were obtained from the slow evaporation of their dichloromethane/hexane solutions (**1a**, **1b**, **1h**, **5d**, **5e**, and **5g**) or the slow diffusion of hexane into their concentrated dichloromethane solutions (**5b**, **5f**, and **5i**). The ORTEP plots of these isoindole BODIPYs are given with thermal ellipsoids at 30% probability level (Figures S1−7 in the Supporting Information). As shown in Figure 4, the plane defined by F−B−F atoms is
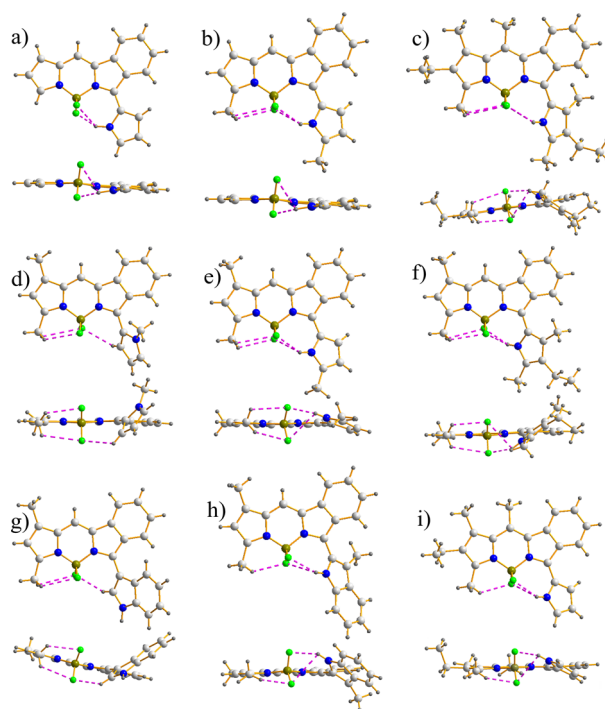
Figure 4. Top and side views of the X-ray structures of isoindole BODIPYs (a) **1a**, (b) **1b**, (c) **1h**, (d) **5b**, (e) **5d**, (f) **5e**, (g) **5f**, (h) **5g**, and (i) **5i**. C, light gray; H, gray; N, blue; B, dark yellow; F, green.

perpendicular to the C_3N_2B core as usual for these isoindole BODIPYs. As summarized in Table S2, the B−N distance for these isoindole BODIPYs is in the range of 1.515−1.577 Å, indicating a usual delocalization of positive charge. All of these isoindole BODIPYs show planar core structures (dihedral angles between 1.8(2) ° and 6.5(2)°) similar to our previously reported isoindole-BODIPYs **1c** and **1f**.[20] A gradual increase of the dihedral angle between uncoordinated pyrrole and the BODIPY core was observed from **1a** (11.6(2) °) to **5d** (22.2(2)°), **1b** (23.9(2)°), **1c** (28.5(2)°), **5i** (31.0(2)°), **5e** (36.5(2)°), and **1h** (41.0(2)°) with the increase of alkyl substitutions onto the uncoordinated pyrrole of these isoindole BODIPYs. A further increase of the dihedral angle was observed in the indole, 3-methylindole, and *N*-methyl-substituted isoindole BODIPYs **5f** (46.6(2)°), **5g** (48.3(2)°), and **5b** (53.1(2)°).

As shown in Figure 4, various hydrogen bondings were observed between fluorine atoms and the hydrogens from uncoordinated

pyrrole and pyrrolic methyl units due to the strong electron negativity of the F atom[23] in these dyes. As summarized in Table S2, the bond distances for these hydrogen bondings is in the range of 1.738−2.850 Å. The various intramolecular and intermolecular hydrogen bonds between the hydrogen of the pyrrolic methyl substituent and the fluorine atoms restrict the free rotation of the 3-pyrrole/indole substituents, enhance the rigidity of these dyes, and form corresponding dimers. The weak interactions between these dimers help to establish crystal packing structures for these isoindole BODIPYs from F and H atoms on aromatic rings and make them nearly parallel to each other in a head-to-head orientation as demonstrated by **1a** and **5b** in Figures S8 and S9, respectively.

Spectroscopic Properties. These isoindole BODIPYs show red to blue color under ambient light and bright red fluorescence upon irradiation by UV light at 365 nm of a hand-held UV lamp in hexane, toluene, dichloromethane, tetrahydrofuran, acetonitrile, and methanol. As summarized in Table 1, all of these isoindole BODIPYs show significantly red-shifted absorption and emission spectra with respect to the BODIPY core (**A**[24]). Among them, isoindole BODIPYs **1** each show fairly good to excellent fluorescence quantum yields (from 0.61 to 0.99) in dichloromethane, except for **1e** (ϕ = 0.08) containing two 3-methylindole moieties. A gradual red-shift was observed from **1a** (570/599 nm) to **1b** (600/624 nm), **1c** (609/631 nm), and **1d** (629/650 nm) with the increase of the alkyl substitutions on the pyrrole rings (Figure 5). This red-shift observed in **1d** (629/650 nm) is even greater than that of indole-containing **1e** (611/648 nm). By contrast, a blue-shift (7−11 nm) was observed when methyl substitution took place at the *meso*-position, as demonstrated by **1f** in Figure 5.

A similar gradual red-shift of the absorption and emission band was also observed from **5a** (602/621 nm) to **5d** (608/629 nm) and **5e** (616/640 nm) with the increase of alkyl substitutions on the uncoordinated pyrrole rings (Figure 6). By contrast, *N*-alkyl substitution leads to a 10−17 nm blue-shift of the spectra with respect to **5a** in dichloromethane as demonstrated by **5b** in Figure 6. As expected, 3-methylindole-substituted **5e** shows an approximate 35 nm red-shift of the spectra in dichloromethane with respect to less conjugated **5f**.

Isoindole BODIPYs **7a−f** show a strong NIR absorption (centered at around 680−725 nm) and emission (centered at around 705−770 nm) in dichloromethane, which is red-shifted with respect to the commercialized BODIPY 650/665 (Figure 1). Among them, **7f** shows an approximate 75 and 105 nm red-shift of the absorption and emission spectra, respectively, in dichloromethane.

Fluorescent decay profiles for isoindole BODIPYs **1**, **5**, and **7** are either a monomeric or a biexponential function with lifetimes in the range of 1.22−8.89 ns in anhydrous dichloromethane (Table 1, Figures S33−75). The fluorescence lifetimes for most of **1** and **5** in dichloromethane are around 5−8.89 ns, similar to most highly fluorescent BODIPYs appearing in the literature.[11d] The comparatively larger nonradiative decay rate constants were observed for **1e** and **7c−e** (7.5 × 10^{8}, 3.2 × 10^{8}, 2.1 × 10^{8}, and 1.3 × 10^{8} s^{−1}, respectively; Table 1) in dichloromethane, which may partially explain the comparatively low fluorescence quantum yields observed in these dyes. These large nonradiative decay rate constants for **7c−e** may be associated with the free rotation of the phenyl moieties in the *meso*-styryl units,[17c,d,25] whereas it is not clear for the large one observed in **1e**.

Solvatochromic Effect. The solvatochromic effects on these isoindole BODIPYs in hexane, toluene, dichloromethane, tetrahydrofuran, acetonitrile, and methanol are summarized in

Table 1. Photophysical Properties of BODIPYs 1, 5, and 7 in Dichloromethane at Room Temperature

dye	λ_{abs}^{max} (nm)[a]	ε (cm^{-1} M^{-1})[b]	λ_{em}^{max} (nm)	Φ[c]	Stokes shift[d] (cm^{-1})	τ[e] (ns)	K_f^f (×10^9 s^{-1})	K_{nr}^g (×10^9 s^{-1})
A[h]	503		512	0.90	349			
1a	570	4.65	599	0.80	849	6.66	0.12	0.03
1b	600	4.46	624	0.79	641	8.11	0.10	0.03
1c	609	4.87	631	0.61	573	6.40	0.10	0.06
1d	629	4.91	650	0.73	514	6.30	0.12	0.04
1e	611	4.99	648	0.08	935	1.22	0.07	0.75
1f	563	4.88	592	0.91	870	6.71	0.14	0.01
1g	599	4.96	625	0.80	694	7.30	0.11	0.03
1h	619	5.07	645	0.72	651	6.21	0.12	0.05
5a	602	4.93	621	0.87	508	7.28	0.12	0.02
5b	585	4.83	611	0.99	727	6.91	0.14	0.001
5c	584	4.72	611	0.99	757	8.89	0.11	0.001
5d	608	4.79	629	0.89	549	6.65	0.13	0.02
5e	616	4.95	640	0.86	609	4.93	0.19	0.01
5f	581	4.89	606	0.98	710	6.42	0.15	0.003
5g	608	4.90	631	0.85	600	3.27	0.26	0.05
5h	616	4.45	634	0.66	461	6.41	0.10	0.05
5i	605	4.85	629	0.92	631	5.75	0.16	0.01
7a	680	4.94	705	0.75	521	5.14	0.15	0.05
7b	675	4.76	714	0.68	809	4.63	0.15	0.07
7c	608	3.92	687	0.014	1891	3.07	0.01	0.32
7d	676	5.16	733	0.012	1150	4.82	0.003	0.21
7e	585	4.63	631	0.003	1246	7.58	0.0004	0.13
7f	725	4.80	770	0.13	806	2.30	0.06	0.38

[a]All of the values correspond to the strongest absorption peaks. [b]Molar absorption coefficients are in the maximum of the highest peak. [c]Fluorescence quantum yields (ϕ) are calculated using Cresyl violet perchlorate (ϕ = 0.54 in methanol) as the reference for **1a–h, 5, 7c**, and **7e** and 1,7-diphenyl-3,5-di(p-methoxyphenyl)-azadipyrromethene (ϕ = 0.36 in chloroform) for **7a, 7b**, and **7d**. Standard errors are less than 10%. [d]Refers to the difference between the absorption and the emission maximum for all dyes. [e]Fluorescence lifetime; standard deviations are less than 0.1 ns. [f]$K_f = \phi/\tau$. [g]$K_{nr} = (1 - \phi)/\tau$. [h]Data taken from ref 24.
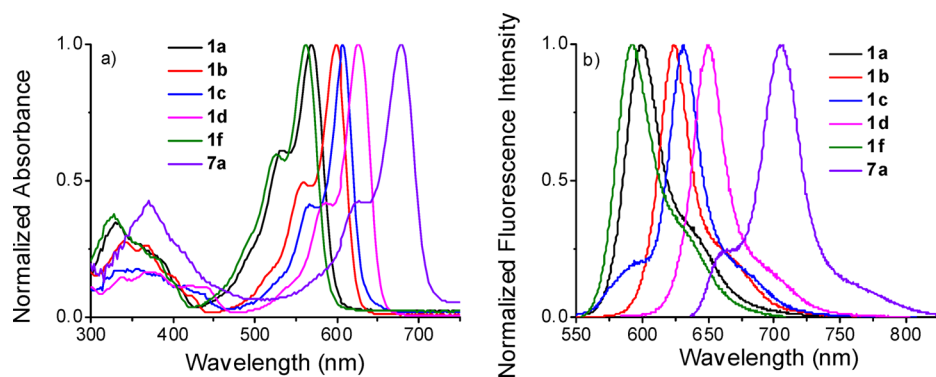

Figure 5. Overlaid and normalized (a) absorption and (b) fluorescence emission spectra of **1a–d, 1f**, and **7a** in dichloromethane.
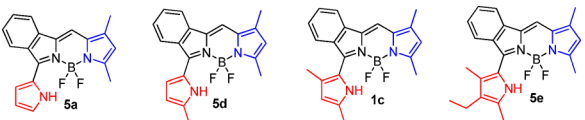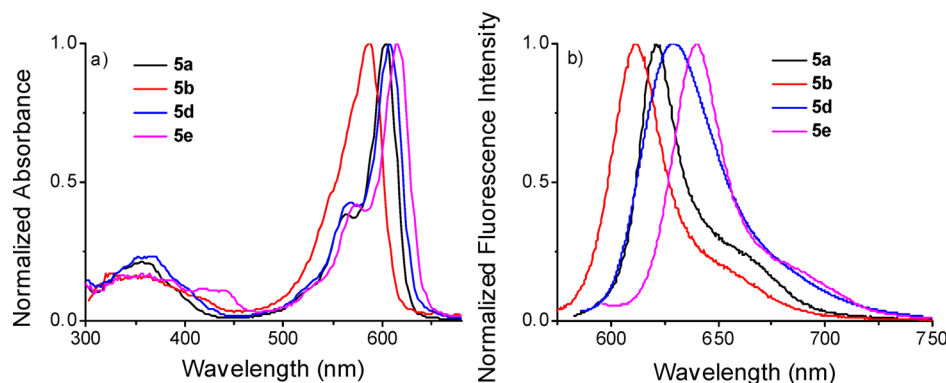

Figure 6. Overlaid and normalized (a) absorption and (b) fluorescence emission spectra of **5a, 5b, 5d**, and **5e** in dichloromethane.

Table 2. Fluorescence Quantum Yields and Lifetimes of 5a, 5d, 1c, and 5e in Hexane, Toluene, Dichloromethane, Tetrahydrofuran, Acetonitrile, and Methanol at Room Temperature

	Φ^a $(\tau)^b$					
dye	hexane	toluene	dichloromethane	tetrahydrofuran	acetonitrile	methanol
5a	0.87 (7.93)	0.78 (6.82)	0.87 (7.28)	0.80 (7.36)	0.85 (7.41)	0.90 (7.47)
5d	0.91 (7.31)	0.83 (6.17)	0.89 (6.65)	0.82 (6.54)	0.84 (6.32)	0.83 (6.50)
1c	0.85 (7.17)	0.81 (6.14)	0.61 (6.40)	0.06 (0.80, 3.75)^c	0.02 (0.56, 4.34)^c	0.03 (0.43, 4.98)^c
5e	0.99 (7.03)	0.99 (5.90)	0.96 (4.93)	0.07 (0.42, 4.41)^c	0.12 (0.26, 5.55)^c	0.14 (0.28, 5.60)^c

^{a}Fluorescence quantum yield (ϕ). ^{b}Monomeric exponential decay fluorescence lifetime (τ). ^{c}Biexponential decay fluorescence lifetime (τ_1, τ_2).
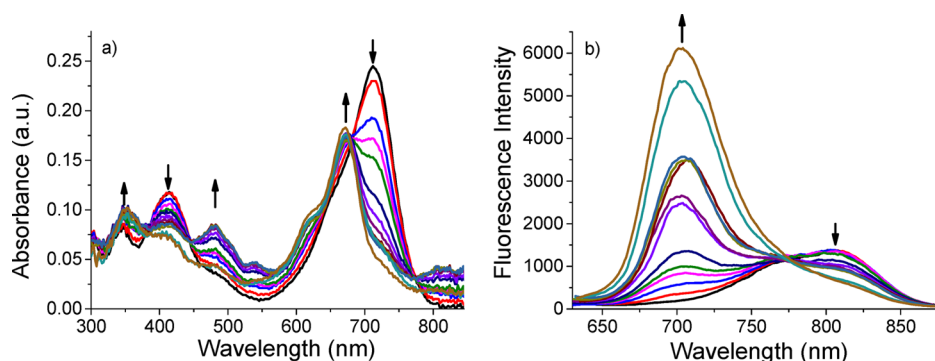

Figure 7. (a) Absorption and (b) fluorescence titration spectra of isoindole BODIPY 7f in acetontrile (5.78×10^{-6} M) with the addition of TFA (6.73×10^{-2} M) from 0 to 230 equiv and excited at 610 nm.

Table S1 and Figures S10–32. For most of these isoindole BODIPYs, increasing the polarity of the solvent only leads to a slight blue-shift of the absorption and emission bands. By contrast, it brings a gradual decrease of the fluorescence quantum yields and dramatic solvent-dependent lifetime decay for those containing a 3-methyl substituent on the uncoordinated pyrrole ring (1c–e, 1g–h, 5e, 5g, and 7a–g). For example, the fluorescence quantum yield for 1c was gradually decreased from 0.85 (hexane) to 0.81 (toluene), 0.61 (dichloromethane), 0.06 (tetrahydrofuran), 0.03 (methanol), and 0.02 (acetonitrile) upon increasing the polarity of the solvent (Table 2). In addition, the fluorescence lifetime decay for 1c (Figure S78) was changed from a monomeric exponential decay to biexponential decay with a significant decrease of the excited-state lifetime: hexane (7.17 ns), toluene (6.14 ns), dichloromethane (6.40 ns), THF ($\tau_1 = 0.80$ ns, $\tau_2 = 3.75$ ns), acetonitrile ($\tau_1 = 0.56$ ns, $\tau_2 = 4.34$ ns), and MeOH ($\tau_1 = 0.43$ ns, $\tau_2 = 4.98$ ns). Similar results were observed for 5e (Table 2 and Figure S79), whereas for 5a and 5d, their fluorescence quantum yields (0.78–0.90 for 5a and 0.82–0.91 for 5d) and fluorescence lifetimes (6.82–7.93 ns for 5a and 6.17–7.31 ns for 5d, Figures S76 and S77) only have slight variations in different solvents. Thus, these isoindole BODIPY dyes may have potential applications as red to NIR environmental sensitive fluorescence probes.[26]

pH-Dependent Absorption and Fluorescence Emission of 7f. Isoindole BODIPY 7f, containing a dimethylamine (NMe_2) moiety, shows strong absorption and weak fluorescence emission in the NIR region in polar solvents like acetonitrile (713/805 nm, $\phi = 0.05$, Table S1) due to the strong intramolecular charge transfer (ICT) process.[27,28] With the addition of trifluoroacetic acid (TFA, 6.73×10^{-2} M), a stepwise

disappearance of the absorption bands at 713 and 415 nm with the appearance of two new bands at 671 and 354 nm was observed for 7f (Figure 7a). The sharp isosbestic point at 680 and 382 nm indicates the formation of a monoprotonated species (7f-H^+). Furthermore, the addition of TFA also causes a blue-shift of the emission band from 805 to 702 nm with an isosbestic point at 774 nm (Figure 7b). This reveals that 7f may be a potential ratiometric "turn-on" NIR fluorescent pH sensor.

Electrochemical Properties. The electronic structures of BODIPYs 1a, 5a, 1c, 1d, and 7f were investigated by cyclic voltammetry (CV) in deoxygenated dichloromethane containing 0.1 M tetrabutylammonium hexafluorophosphate ($TBAPF_6$) as the supporting electrolyte (Figure 8 and Table 3). Among them,
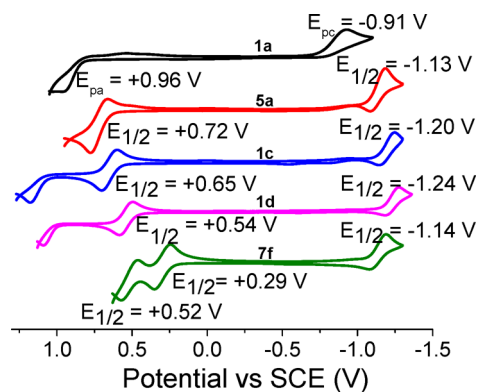

Figure 8. Cyclic voltammograms of 1a, 5a, 1c, 1d, and 7f recorded in dichloromethane containing 0.1 M $TBAPF_6$ at room temperature.

Table 3. Electrochemical Data Acquired and HOMO-LUMO Band Gaps Determined from Spectroscopy of 1a, 5a, 1c, 1d, and 7f[a]

dye	E_{ox}^{1} (V)	E_{ox}^{2} (V)	E_{red} (V)	E_{red}^{onset} (V)	E_{ox}^{onset} (V)	LUMO (eV)	HOMO (eV)	E_g (eV)
1a	0.96		−0.91	−0.81	0.88	−3.59	−5.28	1.69
5a	0.78		−1.19	−1.04	0.62	−3.36	−5.06	1.66
1c	0.70	1.17	−1.23	−1.09	0.56	−3.31	−4.96	1.65
1d	0.58	1.09	−1.27	−1.13	0.46	−3.13	−4.86	1.59
7f	0.35	0.57	−1.19	−1.09	0.25	−3.31	−4.65	1.34

[a]E_{ox}^{1} = the first oxidation peak potential; E_{ox}^{2} = the second oxidation peak potential; E_{red} = the reduction peak potential; E_{red}^{onset} = the onset reduction potential; $E_{LUMO} = -e(E_{red}^{onset} + 4.4)$; E_{ox}^{onset} = the onset oxidation potential; $E_{HOMO} = -e(E_{ox}^{onset} + 4.4)$; $E_g = E_{LUMO} - E_{HOMO}$.

1a exhibits an irreversible reduction wave (E_{pc} at −0.91 V) and an irreversible oxidation wave (E_{pa} at 0.96 V) relative to the saturated calomel electrode (SCE). Similarly, **5a** shows one reversible reduction wave (with half-wave potential at −1.13 V) and one reversible oxidation wave (with half-wave potential at 0.72 V). By contrast, **1c**, **1d**, and **7f** each exhibits two or three reversible waves with half-wave potential values at −1.20/0.65 V, −1.24/0.54 V, and −1.14/0.29/0.52 V, respectively.

On the basis of the onset potential of their first oxidation and reduction waves, the HOMO/LUMO energy levels for **1a**, **5a**, **1c**, **1d**, and **7f** were estimated to be −5.28/−3.59, −5.06/−3.36, −4.96/−3.31, −4.86/−3.13, and −4.65/−3.31 eV, respectively. In comparison with **1d**, **7f** showed an increased HOMO (from −4.86 to −4.65 eV) and a decreased LUMO energy level (from −3.13 to −3.31 eV) with an overall 1.34 eV decrease of the band gap. A gradual increase of the HOMO/LUMO energies and a gradual decrease of the energy band gaps were observed for these isoindole BODIPYs with the increase of the alkyl substitutions on the pyrrole rings. Among them, alkyl substitutions on the coordinated pyrrole unit are more efficient at decreasing the HOMO and LUMO energy levels for these dyes.

DFT Calculations. For a better understanding of the photophysical properties of these dyes, DFT calculations were performed at the B3LYP/6-31G(d) level. As shown in Figure 9,
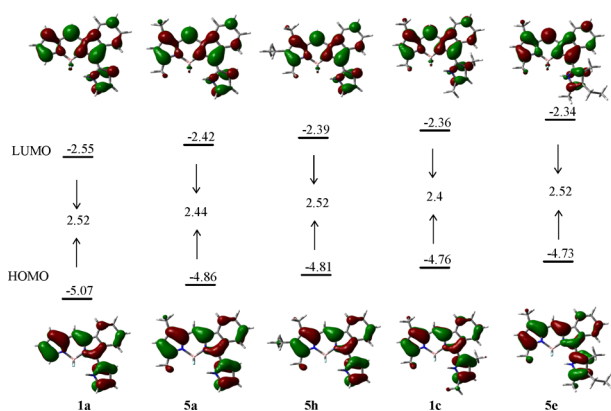

Figure 9. Relative energies of the frontier molecular orbitals (MOs) of **1a**, **1c**, **5a**, **5e**, and **5h**. Calculations are based on ground state geometry by DFT at the B3LYP/6-31G* level.

the HOMO and LUMO were localized over the BODIPY core and the uncoordinated pyrrole rings for **1** and **5**. Increasing alkyl substitutions on pyrrole rings leads to a gradual increase of the HOMO/LUMO energy levels from **1a** (−5.07/−2.55 eV) to **5a** (−4.86/−2.42), **5h** (−4.81/−2.39), **1c** (−4.76/−2.36), and **5e** (−4.73/−2.34 eV). These results of our calculations are in good agreement with electrochemical experimental results.

We further performed time-dependent DFT calculations (TD-DFT) on these dyes in dichloromethane (Table S3).

The calculated absorption maximum (524−562 nm) is blue-shifted with respect to the experimental spectra, similar to the recently reported results.[29] The lowest energy absorption band for these dyes is mainly contributed by HOMO → LUMO transition with high oscillator strength above 0.7, which corresponds to the electronic transition from the ground to the first excited state (S0 → S1).

CONCLUSIONS

In conclusion, we have synthesized a series of isoindole BODIPYs based on either the one-pot condensation of 3-halogenated isoindolylidene with pyrrole/indole derivatives or a two-step reaction between 3-chloro-1-formylisoindole and pyrroles. These dyes show strong absorption and fluorescence emission tunable from the far red to NIR region (up to 805 nm in acetonitrile) via the simple variation of substituents. Most of these dyes show high fluorescence quantum yields (up to 0.99). Solvent-dependent fluorescence emissions were observed for those possessing 3-methyl substituents on the uncoordinated pyrrole unit. X-ray diffraction analysis shows that alkyl and styryl substitution(s) on the pyrrole rings greatly enhanced the dihedral angle between uncoordinated pyrrole and the BODIPY core. Cyclic voltammetry and DFT calculation results indicate that alkyl substitutions on the pyrrole rings increases the HOMO and LUMO energy levels and brings about an overall decrease of the energy band gaps. These isoindole BODIPYs can be further functionalization with a variety of functionalities via Knoevenegal condensation, such as dimethylamine as demonstrated in this work. This dimethylamine-functionalized dye shows weak fluorescence in polar solvents and shows significant potential to be a ratiometric "turn-on" NIR fluorescent pH sensor.

EXPERIMENTAL SECTION

General. Reagents and solvents were used as received from commercial suppliers unless otherwise noted. All reactions were performed in oven-dried or flame-dried glassware unless otherwise stated and were monitored by TLC using 0.25 mm silica gel plates with UV indicator (HSGF 254) for thin-layer chromatography (TLC). Flash column chromatography was performed using silica gel (200−400 mesh). ^{1}H NMR (300 MHz) and ^{13}C NMR (75 MHz) spectra were recorded on a 300 MHz NMR spectrometer in CDCl$_3$. Chemical shifts (δ) are given in ppm relative to CDCl$_3$ (7.26 ppm for ^{1}H and 77 ppm for ^{13}C) or to internal TMS (δ = 0 ppm) as the internal standard. Data are reported as follows: chemical shift, multiplicity, coupling constants, and integration. High-resolution mass spectra (HRMS) were obtained using APCI (or ESI or EI)-TOF in positive mode. BODIPYs **5a** and **7a−e** were synthesized using the procedures described in our previous communication.[20]

Compounds 2a and 2b Synthesized Using a Modified Literature Method.[30] Compound **2a**: To a solution of POCl$_3$ (3.2 mL, 30 mmol) in anhydrous dichloromethane (7 mL) at 0 °C was dropwise added *N,N*-dimethylformamide (DMF, 2.6 mL, 30 mmol) in anhydrous dichloromethane (15 mL). The reaction mixture was stirred for 30 min at room temperature. To the reaction mixture was slowly added 1H-isoindolinone

1 (2 g, 15 mmol) in 80 mL of dichloromethane. It was heated at reflux for 4.5 h, neutralized with an ice-cold aqueous solution of Na_2CO_3 (2 M), extracted with dichloromethane, filtered, and dried over anhydrous Na_2SO_4. The solvent was removed under a vacuum. The residue was purified by silica gel chromatography (petroleum/ethyl acetate = 4:1, v/v) to give **2a** as white crystals in 47% yield (1.45 g). ^{1}H NMR (300 MHz, CDCl$_3$): δ 7.62 (d, J = 7.8 Hz, 1H), 7.57 (d, J = 7.8 Hz, 1H), 7.30 (t, J = 7.8 Hz, 1H), 7.24−7.17 (m, 2H), 3.58 (s, 3H), 3.33 (s, 3H).

Compound **2b** was obtained in 45% yield (1.49 g) as a white solid from dimethylacetamide (2.8 mL, 30 mmol) using the procedure for **2a**. ^{1}H NMR (300 MHz, CDCl$_3$): δ 7.66−7.64 (m, 2H), 7.32 (t, J = 4.5 Hz, 1H), 7.20 (t, J = 7.5 Hz, 2H), 3.46 (s, 6H), 2.69 (s, 3H).

*Compounds **3a** and **3b** Synthesized Using a Modified Literature Procedure.*[30] Compound **3a:** To **2a** (1.03 g, 5 mmol) in 100 mL of ethanol was added NaOH (4 M, 6 mL). The reaction mixture was refluxed for 3 h, cooled to room temperature, and concentrated. Then, the solution was neutralized with HCl (3 M) to tune the pH to 7, extracted with dichloromethane (3 × 80 mL), filtered, and dried over anhydrous Na_2SO_4. The solvent was removed under a vacuum. The residue was recrystallized from MeOH/H$_2$O (1:3) to give **3a** as white crystals in 85% yield (760 mg). ^{1}H NMR (300 MHz, CDCl$_3$): δ 9.73 (s, 1H), 7.93 (d, J = 8.4 Hz, 1H), 7.70 (d, J = 8.4 Hz, 1H), 7.43 (t, J = 7.8 Hz, 1H), 7.26 (t, J = 7.5 Hz, 1H).

Compound **3b** was obtained as a white solid in 80% yield (702 mg) from **2b** (1.0 g, 4.5 mmol) using the procedure for **3a** and was purified by recrystallization in MeOH/H$_2$O (1:3 v/v). ^{1}H NMR (300 MHz, CDCl$_3$): δ 7.86 (d, J = 8.7 Hz, 1H), 7.66 (d, J = 7.8 Hz, 1H), 7.38 (t, J = 7.2 Hz, 1H), 7.18 (t, J = 7.8 Hz, 1H), 2.72 (s, 3H).

General Procedure for the Preparation of Isoindole BODIPYs 1. To the mixture of compound **2a** (0.5 mmol) and pyrrole derivatives (10 mmol) in 60 mL of 1,2-dichloroethane (or the mixture of 1,2-dichloroethane and toluene, 1:1 v/v) was added POCl$_3$ (0.47 mL, 5 mmol) in ice-cold conditions under argon. The reaction mixture was stirred under refluxing conditions and monitored by TLC. Upon completion of the reaction, Et$_3$N (1.5 mL) was added to the reaction mixture under ice-cold conditions, and the mixture was left to stir for an additional 10 min before adding BF$_3$·OEt$_2$ (2.5 mL) under ice-cold conditions through a syringe. The reaction mixture was left stirring overnight, poured into water, and extracted with CH$_2$Cl$_2$ (3 × 60 mL). The organic layers were combined, and the solvent was removed under vacuum. The crude product was purified by silica gel chromatography (petroleum/CH$_2$Cl$_2$ = 2:1 v/v) to afford the desired compound as a bluish (or reddish or greenish) powder.

Compound **1a**[20] was obtained as a reddish powder in 24% yield (37 mg) from **2a** (103 mg, 0.5 mmol) and pyrrole (0.69 mL, 10 mmol) in a mixture of 1,2-dichloroethane and toluene (1:1 v/v) at 110 °C for 10 h. ^{1}H NMR (300 MHz, CDCl$_3$): δ 10.11 (s, 1H), 7.95 (d, J = 7.2 Hz, 1H), 7.75 (d, J = 7.2 Hz, 1H), 7.41−7.31 (m, 2H), 7.14 (s, 1H), 7.02 (s, 1H), 6.90 (s, 1H), 6.80 (s, 1H), 6.50 (s, 1H), 6.31 (s, 1H), 6.14 (s, 1H).

Compound **1b**[20] was obtained as bluish powder in 38% yield (64 mg) from **2a** (103 mg, 0.5 mmol) and 2-methylpyrrole (0.42 mL, 5 mmol) in 1,2-dichloroethane for 40 min. ^{1}H NMR (300 MHz, CDCl$_3$): δ 10.59 (s, 1H), 8.12 (d, J = 7.8 Hz, 1H), 7.78 (d, J = 7.5 Hz, 1H), 7.54 (t, J = 7.5 Hz, 1H), 7.40 (t, J = 7.8, 1H), 7.19 (s, 1H), 6.64 (s, 1H), 6.24 (s, 1H), 6.13 (s, 1H), 2.59 (s, 3H), 2.50 (s, 3H).

Compound **1c**[20] was obtained as a bluish powder in 52% yield (94 mg) from **2a** (103 mg, 0.5 mmol) and 2,4-dimethylpyrrole (0.5 mL, 5 mmol) in 1,2-dichloroethane for 40 min. ^{1}H NMR (300 MHz, CDCl$_3$): δ 9.70 (s, 1H), 7.83−7.77 (m, 2H), 7.49 (d, J = 7.2 Hz, 1H), 7.34−7.28 (m, 2H), 6.03 (s, 1H), 5.99 (s, 1H), 2.50 (s, 3H), 2.40 (s, 3H), 2.30 (s, 3H), 2.29 (s, 3H).

Compound **1d**[20] was obtained as a greenish powder in 47% yield (99 mg) from **2a** (103 mg, 0.5 mmol) and 2,4-dimethyl-3-ethylpyrrole (0.65 mL, 5 mmol) in 1,2-dichloroethane for 40 min. ^{1}H NMR (300 MHz, CDCl$_3$): δ 9.64 (s, 1H), 7.81−7.74 (m, 2H), 7.46 (d, J = 7.2 Hz, 1H), 7.31−7.13 (m, 2H), 2.53−2.37 (m, 7H), 2.35 (s, 3H), 2.25 (s, 3H), 2.22 (s, 3H), 1.16 (t, J = 7.5 Hz, 3H), 1.09 (t, J = 7.5 Hz, 3H).

Compound **1e**[20] was obtained as a brown powder in 20% yield (44 mg) from **2a** (103 mg, 0.5 mmol) and 3-methylindole (1.2 g, 9.2 mmol)

in a mixture of ClCH$_2$CH$_2$Cl and toluene (1:1 v/v) at 110 °C for 10 h. ^{1}H NMR (300 MHz, CDCl$_3$): δ 10.06 (s, 1H), 8.00 (d, J = 4.2 Hz, 1H), 7.89 (d, J = 7.2 Hz, 1H), 7.72−7.66 (m, 4H), 7.54−7.53 (m, 2H), 7.42−7.37 (t, J = 6.6 Hz, 1H), 7.29−7.21 (m, 3H), 7.06 (s, 1H), 2.61−2.59 (m, 6H).

Compound **1f**[20] was obtained as a reddish powder in 22% yield (35 mg) from **2b** (110 mg, 0.5 mmol) and pyrrole (0.69 mL, 10 mmol) in a mixture of ClCH$_2$CH$_2$Cl and toluene (1:1 v/v) at 110 °C for 10 h. ^{1}H NMR (300 MHz, CDCl$_3$): δ 10.80 (s, 1H), 8.19 (d, J = 7.8 Hz, 1H), 8.00 (d, J = 7.8 Hz, 1H), 7.59 (t, J = 7.5 Hz, 1H), 7.48−7.41 (m, 2H), 7.34−7.30 (m, 2H), 6.90 (s, 1H), 6.51 (s, 1H), 6.43 (s, 1H), 2.76 (s, 3H).

Compound **1g**[20] was obtained as a bluish powder in 43% yield (81 mg) from **2b** (110 mg, 0.5 mmol) and 2,4-dimethylpyrrole (0.5 mL, 5 mmol) in 1,2-dichloroethane for 40 min. ^{1}H NMR (300 MHz, CDCl$_3$): δ 9.52 (s, 1H), 8.00 (d, J = 8.1 Hz, 1H), 7.78 (d, J = 8.1 Hz, 1H), 7.49 (t, J = 7.5 Hz, 1H), 7.30 (t, J = 7.5 Hz, 1H), 6.01−5.98 (m, 2H), 2.85 (s, 3H), 2.48 (s, 3H), 2.46 (s, 3H), 2.38 (s, 3H), 2.23 (s, 3H).

Compound **1h**[20] was obtained as a greenish powder in 42% yield (91 mg) from **2b** (110 mg, 0.5 mmol) and 2,4-dimethy-3-ethylpyrrole (0.65 mL, 5 mmol) in 1,2-dichloroethane for 40 min. ^{1}H NMR (300 MHz, CDCl$_3$): δ 9.46 (s, 1H), 8.00 (d, J = 8.4 Hz, 1H), 7.76 (d, J = 8.1 Hz, 1H), 7.46 (t, J = 7.8 Hz, 1H), 7.30−7.26 (t, J = 7.8 Hz, 1H), 2.88 (s, 3H), 2.53−2.40 (m, 10H), 2.34 (s, 3H), 2.18 (s, 3H), 1.17 (t, J = 7.2 Hz, 3H), 1.06 (t, J = 7.2 Hz, 3H).

Compound **6a** was used as an example to demonstrate the general procedure for the preparation of dipyrromethene **6**: To compound **3a** (179 mg, 1 mmol) in 60 mL of dichloromethane were added 2,4-dimethylpyrrole (103 μL, 1 mmol) in 1 mL of CH$_2$Cl$_2$ and POCl$_3$ (94 μL, 1 mmol) in 1 mL of CH$_2$Cl$_2$ in ice-cold conditions under argon. The reaction mixture was stirred in ice-cold conditions for 30 min and was followed by TLC. Upon completion of the reaction, the reaction mixture was quenched by triethylamine (1.2 mL), poured into water, and extracted with dichloromethane (3 × 80 mL). Organic layers were combined and dried over anhydrous Na_2SO_4. The solvent was removed under vacuum. The crude product was purified by silica gel chromatography (petroleum/dichloromethane = 2:1 v/v) to afford desired compound **6a** as a reddish powder in 90% yield (230 mg). ^{1}H NMR (300 MHz, CDCl$_3$): δ 10.78 (s, 1H), 7.73 (d, J = 6.0 Hz, 1H), 7.59 (d, J = 6.0 Hz, 1H), 7.41 (t, J = 6.0 Hz, 1H), 7.30 (t, J = 6.0 Hz, 1H), 7.07 (s, 1H), 5.85 (s, 1H), 2.35 (s, 3H), 2.25 (s, 3H). ^{13}C NMR (75 MHz, CDCl$_3$): δ 152.8, 140.3, 138.4, 137.6, 133.1, 130.8, 128.5, 127.2, 125.9, 120.5, 118.7, 114.8, 111.6, 13.9, 11.4. HRMS (EI) calcd for C$_{15}$H$_{13}$N$_2$Cl [M]$^+$: 256.0767, found 256.0774.

Compound **6b** was obtained as a reddish powder in 83% yield (212 mg) from **3a** (179 mg, 1 mmol) and 2,4-dimethyl-3-ethylpyrrole (135 μL, 1 mmol). ^{1}H NMR (300 MHz, CDCl$_3$): δ 10.67 (s, 1H), 7.67 (d, J = 6.0 Hz, 1H), 7.53 (d, J = 6.0 Hz, 1H), 7.33 (t, J = 6.0 Hz, 1H), 7.23 (t, J = 6.0 Hz, 1H), 7.01 (s, 1H), 2.35 (q, J = 6.0 Hz, 2H), 2.25 (s, 3H), 2.14 (s, 3H), 1.00 (t, J = 6.0 Hz, 3H).^{13}C NMR (75 MHz, CDCl$_3$): δ 152.0, 140.3, 138.0, 135.1, 132.8, 128.9, 128.3, 126.2, 125.6, 124.6, 120.4, 118.6, 114.8, 17.4, 15.3, 12.0, 9.5. HRMS (EI) calcd for C$_{17}$H$_{17}$N$_2$Cl [M]$^+$: 284.1080, found 284.1079.

Compound **6c** was obtained as a reddish powder in 79% yield (235 mg) from **3b** (193 mg, 1 mmol) and 2,4-dimethyl-3-ethylpyrrole (135 μL, 1 mmol). ^{1}H NMR (300 MHz, CDCl$_3$): δ 12.23 (s, 1H), 7.91 (d, J = 6.0 Hz, 1H), 7.64 (d, J = 6.0 Hz, 1H), 7.41 (t, J = 6.0 Hz, 1H), 7.30 (t, J = 6.0 Hz, 1H), 2.81 (s, 3H), 2.45−2.32 (m, 8H), 1.06 (t, J = 6.0 Hz, 3H). ^{13}C NMR (75 MHz, CDCl$_3$): δ 149.0, 139.4, 137.9, 135.6, 133.4, 133.3, 128.3, 127.8, 127.7, 125.5, 125.0, 122.8, 120.9, 18.5, 17.3, 15.5, 13.6, 12.0. HRMS (EI) calcd for C$_{18}$H$_{19}$N$_2$Cl [M]$^+$: 298.1237, found 298.1245.

General Procedure for the Preparation of Isoindole BODIPYs 5. To compound **6** (0.5 mmol) in 60 mL of 1,2-dichloroethane were added suitable pyrrole or indole derivatives (10 mmol) in 1 mL of 1,2-dichloroethane and POCl$_3$ (0.47 mL, 5 mmol) in 1 mL of 1,2-dichloroethane at ice-cold conditions under argon. The reaction mixture was stirred at varying temperatures (from 35 °C to refluxing temperature) depending on the reactivity of the pyrrole or indole derivatives and was followed by TLC. Upon completion of the reaction, triethylamine (1.5 mL) was added to the reaction mixture under ice-cold

conditions. The reaction mixture was further stirred for an additional 10 min before adding BF$_3$·OEt$_2$ (2.5 mL) under ice-cold conditions through a syringe. The reaction mixture was left stirring for 2 h, poured into water, and extracted with dichloromethane (3 × 80 mL). The organic layers were combined, and the solvent was removed under vacuum. The crude product was purified by silica gel chromatography (petroleum/CH$_2$Cl$_2$ = 2:1 v/v) to afford the desired compound as a reddish or greenish powder.

Compound **5b** was obtained as a reddish powder in 30% yield (52 mg) from **6a** (128 mg, 0.5 mmol) and *N*-methylpyrrole (0.94 mL, 10 mmol) at refluxing conditions for 10 h. ^{1}H NMR (300 MHz, CDCl$_3$): δ 7.85 (d, *J* = 4.5 Hz, 1H), 7.53−7.45 (m, 2H), 7.41 (s, 1H), 7.29 (t, *J* = 6.0 Hz, 1H), 6.94 (s, 1H), 6.83 (s, 1H), 6.39 (s, 1H), 6.01 (s, 1H), 3.58 (s, 3H), 2.49 (s, 3H), 2.30 (s, 3H). ^{13}C NMR (75 MHz, CDCl$_3$): δ 153.6, 146.1, 138.3, 134.9, 132.3, 131.7, 129.6, 128.9, 126.6, 125.7, 123.8, 123.3, 119.0, 117.9, 116.7, 115.8, 109.3, 35.6, 14.6, 11.3. HRMS (APCI) calcd for C$_{20}$H$_{19}$N$_3$BF$_2$ [M + H]$^+$: 350.1636, found 350.1635.

Compound **5c** was obtained as a gray powder in 38% yield (92 mg) from **6a** (128 mg, 0.5 mmol) and *N*-undecylpyrrole (2.21 g, 10 mmol) at refluxing conditions for 10 h. ^{1}H NMR (300 MHz, CDCl$_3$): δ 7.85 (d, *J* = 4.5 Hz, 1H), 7.54−7.46 (m, 2H), 7.40 (s, 1H), 7.31 (d, *J* = 4.5 Hz, 1H), 7.00 (s, 1H), 6.84 (s, 1H), 6.39 (t, *J* = 3.0 Hz, 1H), 6.02 (s, 1H), 3.98−9.84 (m, 2H), 2.49 (s, 3H), 2.31 (s, 3H), 1.33−1.05 (m, 18H), 0.86 (t, *J* = 6.0 Hz, 3H). ^{13}C NMR (75 MHz, CDCl$_3$): δ 153.3, 146.7, 137.9, 135.0, 132.1, 131.6, 129.6, 129.0, 125.7, 125.5, 123.9, 122.8, 119.0, 117.7, 116.5, 116.1, 109.4, 48.8, 31.9, 31.6, 29.5, 29.3, 28.9, 26.3, 22.6, 14.7, 14.1, 11.3. HRMS (APCI) calcd for C$_{30}$H$_{39}$N$_3$BF$_2$ [M + H]$^+$: 490.3200, found 490.3190.

Compound **5d** was obtained as a bluish powder in 47% yield (82 mg) from **6a** (128 mg, 0.5 mmol) and distilled 2-methylpyrrole (0.81 g, 10 mmol) at 35 °C for 1 h. ^{1}H NMR (300 MHz, CDCl$_3$): δ 10.52 (s, 1H), 8.11 (d, *J* = 4.5 Hz, 1H), 7.81 (d, *J* = 4.5 Hz, 1H), 7.51 (t, *J* = 6.0 Hz, 1H), 7.39−7.29 (m, 2H), 7.21 (s, 1H), 6.21 (s, 1H), 5.98 (s, 1H), 2.54 (s, 3H), 2.49 (s, 3H), 2.27 (s, 3H). ^{13}C NMR (75 MHz, CDCl$_3$): δ 147.4, 146.2, 137.3, 136.1, 132.9, 130.8, 130.6, 130.4, 129.9, 126.4, 124.6, 121.5, 120.0, 119.1, 116.1, 112.1, 111.0, 14.3, 13.8, 11.1. HRMS (APCI) calcd for C$_{20}$H$_{19}$N$_3$BF$_2$ [M + H]$^+$: 350.1635, found 350.1634.

Compound **5e** was obtained as a greenish powder in 54% yield (105 mg) from **6a** (128 mg, 0.5 mmol) and 3-ethyl-2,4-dimethylpyrrole (0.65 mL, 5 mmol) at 35 °C for 10 min. ^{1}H NMR (300 MHz, CDCl$_3$): δ 9.69 (s, 1H), 7.80 (t, *J* = 6.0 Hz, 2H), 7.49 (t, *J* = 6.0 Hz, 1H), 7.32 (t, *J* = 6.0 Hz, 1H), 7.25 (s, 1H), 5.98 (s, 1H), 2.53−2.45 (m, 5H), 2.36 (s, 3H), 2.28 (s, 3H), 2.26 (s, 3H), 1.16 (t, *J* = 6.0 Hz, 3H). ^{13}C NMR (75 MHz, CDCl$_3$): δ 148.5, 147.9, 136.1, 133.8, 131.7, 131.2, 130.7, 130.6, 129.9, 125.9, 125.5, 125.4, 118.9, 117.7, 116.3, 112.9, 17.8, 15.1, 14.3, 12.9, 11.9, 11.2. HRMS (APCI) calcd for C$_{23}$H$_{25}$N$_3$BF$_2$ [M + H]$^+$: 392.2104, found 392.2098.

Compound **5f** was obtained as a greenish powder in 29% yield (55 mg) from **6a** (128 mg, 0.5 mmol) and indole (1.17 g, 10 mmol) at refluxing conditions for 12 h. ^{1}H NMR (300 MHz, CDCl$_3$): δ 8.81 (s, 1H), 8.24 (s, 1H), 7.87 (d, *J* = 9.0 Hz, 2H), 7.69 (d, *J* = 4.5 Hz, 1H), 7.53 (t, *J* = 9.0 Hz, 1H), 7.43−7.27 (m, 2H), 7.25−7.14 (m, 3H), 6.00 (s, 1H), 2.49 (s, 3H), 2.31 (s, 3H). ^{13}C NMR (75 MHz, CDCl$_3$): δ 151.9, 150.4, 136.2, 136.0, 135.8, 131.8, 131.2, 130.1, 130.0, 129.6, 129.4, 129.3, 126.5, 125.4, 123.0, 120.9, 119.0, 116.9, 115.1, 111.8, 107.4, 14.5, 11.3. HRMS (APCI) calcd for C$_{23}$H$_{19}$N$_3$BF$_2$ [M + H]$^+$: 386.1635, found 386.1631.

Compound **5g** was obtained as a bluish powder in 40% yield (79 mg) from **6a** (128 mg, 0.5 mmol) and 3-methylindole (1.31 g, 10 mmol) at refluxing conditions for 12 h. ^{1}H NMR (300 MHz, CDCl$_3$): δ 9.61 (s, 1H), 7.88 (d, *J* = 4.5 Hz, 1H), 7.75 (d, *J* = 3.0 Hz, 1H), 7.69 (d, *J* = 3.0 Hz, 1H), 7.52 (t, *J* = 9.0 Hz, 2H), 7.43 (s, 1H), 7.38−7.30 (m, 2H), 7.18 (s, 1H), 6.06 (s, 1H), 2.51 (s, 6H), 2.33 (s, 3H). ^{13}C NMR (75 MHz, CDCl$_3$): δ 162.7, 153.5, 145.6, 138.4, 137.3, 135.4, 132.3, 131.1, 129.8, 129.1, 125.8, 125.1, 124.4, 124.2, 119.8, 119.0, 118.1, 116.5, 116.2, 111.8, 14.6, 11.7, 11.4. HRMS (ESI) calcd for C$_{24}$H$_{21}$N$_3$BF$_2$ [M + H]$^+$: 400.1791, found 400.1788.

Compound **5h** was obtained as a reddish powder in 43% yield (78 mg) from **6b** (142 mg, 0.5 mmol) and pyrrole (0.69 mL, 10 mmol) at 35 °C for 8 h. ^{1}H NMR (300 MHz, CDCl$_3$): δ 10.71 (s, 1H), 8.12 (d, *J* = 3.0 Hz, 1H), 7.82 (d, *J* = 3.0 Hz, 1H), 7.49 (d, *J* = 3.0 Hz, 1H), 7.38−7.30 (m, 4H), 6.49 (s, 1H), 2.52−2.41 (m, 5H), 2.23 (s, 3H), 1.10 (t, *J* = 6.0 Hz, 3H). ^{13}C NMR (75 MHz, CDCl$_3$): δ 147.7, 145.1, 141.5, 135.8, 132.4, 130.4, 130.3, 129.9, 129.7, 126.1, 124.9, 124.5, 122.7, 119.0, 117.5, 113.3, 111.4, 17.4, 14.9, 12.2, 9.5. HRMS (EI) calcd for C$_{21}$H$_{20}$N$_3$BF$_2$ [M]$^+$: 363.1718, found 363.1723.

Compound **5i** was obtained as a reddish powder in 42% yield (79 mg) from **6c** (150 mg, 0.5 mmol) and pyrrole (0.69 mL, 10 mmol) at 35 °C for 8 h. ^{1}H NMR (300 MHz, CDCl$_3$): δ 10.60 (s, 1H), 8.15 (d, *J* = 4.5 Hz, 1H), 7.99 (d, *J* = 3.0 Hz, 1H), 7.48 (m, 1H), 7.32−7.25 (m, 1H), 7.20−7.16 (m, 2H), 6.47 (s, 1H), 2.85 (s, 3H), 2.50−2.39 (m, 8H), 1.07 (t, *J* = 6.0 Hz, 3H). ^{13}C NMR (75 MHz, CDCl$_3$): δ 146.2, 143.7, 135.2, 134.4, 132.6, 130.9, 130.0, 129.8, 128.3, 125.1, 125.0, 123.8, 122.4, 122.1, 116.8, 110.8, 17.2, 16.9, 15.2, 13.8, 12.1. HRMS (EI) calcd for C$_{22}$H$_{22}$N$_3$BF$_2$ [M]$^+$: 377.1875, found 377.1883.

Compound **7f**: To 4-(dimethylamino)benzaldehyde **8** (90 mg, 0.6 mol) and **1d** (126 mg, 0.33 mmol) in 20 mL of toluene were added piperidine (1.5 mL) through a syringe and a crystal of *p*-TsOH. The reaction mixture was left at 140 °C for 14 h. Water was removed with a Soxhlet extractor containing anhydrous CaCl$_2$. The reaction was monitored by TLC. Upon the disappearence of **1d**, the reaction mixture was cooled to room temperature, poured into water, and extracted with dichloromethane (3 × 50 mL). Organic layers were combined and dried over anhydrous Na$_2$SO$_4$. Solvent was removed under vacuum. The crude product was purified by chromatography (petroleum/ dichloromethane = 1:1 v/v) and washed with CH$_3$OH to afford **7f** as a gray powder in 30% yield (54 mg). ^{1}H NMR (300 MHz, CDCl$_3$): δ 9.74 (s, 1H), 7.76−7.74 (m, 2H), 7.44−7.39 (m, 4H), 7.27−7.17 (m, 3H), 6.70 (d, *J* = 3.0 Hz, 1H), 2.99 (m, 5H), 2.68−2.21 (m, 13H), 1.23−1.17 (m, 6H). ^{13}C NMR (75 MHz, CDCl$_3$): δ 150.3, 146.1, 135.1, 133.2, 130.8, 129.2, 128.2, 126.4, 125.6, 125.2, 124.6, 119.1, 118.0, 115.9, 112.3, 40.4, 18.8, 17.8, 15.2, 14.2, 12.8, 11.9, 9.1. HRMS (APCI) calcd for C$_{34}$H$_{37}$N$_4$BF$_2$ [M + H]$^+$: 551.3158, found 551.3154.

Photophysical Measurements. UV−visible absorption and fluorescence emission spectra were recorded on commercial spectrophotometers (190−870 nm scan range) at room temperature (10 mm quartz cuvette). Relative fluorescence quantum efficiencies of BODIPY derivatives were obtained by comparing the areas under the corrected emission spectrum of the test sample in various organic solvents with Cresyl violet perchlorate (ϕ = 0.54 in anhydrous methanol)[31] and 1,7-diphenyl-3,5-di(*p*-methoxyphenyl)-azadipyrromethene (ϕ = 0.36 in chloroform).[32] Nondegassed, spectroscopic grade solvents and a 10 mm quartz cuvette were used. Dilute solutions (0.01 < A < 0.05) were used to minimize the reabsorption effects. Quantum yields were determined using the equation[33]

$$\Phi_x = \Phi_r \times \frac{F_x}{F_r} \times \frac{1 - 10^{-A_r(\lambda_{ex})}}{1 - 10^{-A_x(\lambda_{ex})}} \times \frac{n_x^2}{n_r^2}$$

where the subscripts *x* and *r* refer to our sample *x* and reference (standard) fluorophore *r* with known quantum yield Φ_r in a specific solvent, *F* stands for the spectrally corrected, integrated fluorescence spectra, $A(\lambda_{ex})$ denotes the absorbance at the used excitation wavelength λ_{ex}, and *n* represents the refractive index of the solvent (in principle at the average emission wavelength).

Fluorescence lifetimes (τ) of the S1 state were measured by the time-correlated single photon counting method on a commercial steady-state lifetime fluorescence spectrometer with corresponding excitation and emission monitored at the peak maximum. The fluorescence lifetime values were obtained from deconvolution and distribution lifetime analysis. When the fluorescence decays were single exponential, the rate constants of radiative (k_f) and nonradiative (k_{nr}) deactivation were calculated from the measured fluorescence quantum yield and fluorescence lifetime in dichloromethane using the equations $k_f = \phi/\tau$ and $k_{nr} = (1 − \phi)/\tau$.

Crystallography. Crystal diffraction of BODIPYs **1a**, **1b**, **1h**, **5b**, **5d**, **5e**, **5f**, **5g**, and **5i** suitable for X-ray analysis was performed on a CCD

diffractometer using graphite-monochromated Mo Kα radiation ($\lambda = 0.71073$ Å) at 293(2) K with φ and ω scan techniques. An empirical absorption correction was applied using the SADABS program.[34] All structures were solved by direct methods, completed by subsequent difference Fourier syntheses, and refined anisotropically for all non-hydrogen atoms by full-matrix least-squares calculations based on F^2 using the SHELXTL program package.[35] The hydrogen atom coordinates were calculated with SHELXTL by using an appropriate riding model with varied thermal parameters. The residual electron densities were of no chemical significance. Crystals of BODIPYs **1a** (CCDC 978648), **1b** (CCDC 1055531), **1h** (CCDC 1055368), **5b** (CCDC 1003315), **5d** (CCDC 979479), **5e** (CCDC 978647), **5f** (CCDC 978651), **5g** (CCDC 978650), and **5i** (CCDC 978674) contain the supplementary crystallographic data for this paper. These data can be obtained free of charge from The Cambridge Crystallographic Data Centre via www.ccdc.cam.ac.uk/data_request/cif.

Electrochemistry. Electrochemical cells used for the cyclic voltammetry experiment consisted of a three-electrode setup including a glassy carbon as working electrode, platinum wire as counter electrode, and saturated calomel electrode (SCE) as the pseudo-reference electrode. Experiments were run at 20 mV s^{-1} scan rates in degassed dichloromethane solutions of the analytes (∼1 mM) and supporting electrolyte (0.1 M tetrabutylammonium hexafluorophosphate) at room temperature. Cyclic voltammograms were referenced against an external standard (∼1 mM potassium ferricyanide) and corrected for external cell resistance.

Computational Details. All of the calculations were carried out by methods implemented in the Gaussian 09 package.[36] The ground state geometry was optimized by using the DFT method at B3LYP/6-31G (d) level. The same method was used for vibrational analysis to verify that the optimized structures correspond to local minima on the energy surface. TD-DFT computations were used to obtain the vertical excitation energies and oscillator strengths at the optimized ground state equilibrium geometries under the B3LYP/6-31+G (d) theoretical level. TD-DFT calculated molecules in dichloromethane were determined using the self-consistent reaction field method and polarizable continuum model.

■ ASSOCIATED CONTENT

Ⓢ Supporting Information

The Supporting Information is available free of charge on the ACS Publications website at DOI: 10.1021/acs.joc.6b00414.

> Crystal structure data, additional photophysical data and spectra, copies of NMR spectra and high resolution mass spectra for all new compounds, calculated frontier orbitals, and absorption spectra (PDF)
> Crystallographic data for compound **1a** (CIF)
> Crystallographic data for compound **1b** (CIF)
> Crystallographic data for compound **1h** (CIF)
> Crystallographic data for compound **5b** (CIF)
> Crystallographic data for compound **5d** (CIF)
> Crystallographic data for compound **5e** (CIF)
> Crystallographic data for compound **5f** (CIF)
> Crystallographic data for compound **5g** (CIF)
> Crystallographic data for compound **5i** (CIF)

■ AUTHOR INFORMATION

Corresponding Authors
*E-mail: haoehong@ahnu.edu.cn.
*E-mail: jiao421@ahnu.edu.cn.

Notes
The authors declare no competing financial interest.

■ ACKNOWLEDGMENTS

■ REFERENCES

(1) (a) Rudin, M.; Weissleder, R. *Nat. Rev. Drug Discov.* **2003**, *2*, 123−131. (b) Escobedo, J. O.; Rusin, O.; Lim, S.; Strongin, R. M. *Curr. Opin. Chem. Biol.* **2010**, *14*, 64−70. (c) Holzhauser, C.; Wagenknecht, H.-A. *J. Org. Chem.* **2013**, *78*, 7373−7379. (d) Meares, A.; Satraitis, A.; Santhanam, N.; Yu, Z.; Ptaszek, M. *J. Org. Chem.* **2015**, *80*, 3858−3869.

(2) (a) Umezawa, K.; Nakamura, Y.; Makino, H.; Citterio, D.; Suzuki, K. *J. Am. Chem. Soc.* **2008**, *130*, 1550−1551. (b) Yang, Y.; Lowry, M.; Xu, X.; Escobedo, J. O.; Sibrian-Vazquez, M.; Wong, L.; Schowalter, C. M.; Jensen, T. J.; Fronczek, F. R.; Warner, I. M.; Strongin, R. M. *Proc. Natl. Acad. Sci. U. S. A.* **2008**, *105*, 8829−8834. (c) McCann, T. E.; Kosaka, N.; Koide, Y.; Mitsunaga, M.; Choyke, P. L.; Nagano, T.; Urano, Y.; Kobayashi, H. *Bioconjugate Chem.* **2011**, *22*, 2531−2538.

(3) (a) Loudet, A.; Burgess, K. *Chem. Rev.* **2007**, *107*, 4891−4932. (b) Ulrich, G.; Ziessel, R.; Harriman, A. *Angew. Chem., Int. Ed.* **2008**, *47*, 1184−1201.

(4) (a) Golf, H. R.; Reissig, H.; Wiehe, A. *Org. Lett.* **2015**, *17*, 982−985. (b) Golf, H. R.; Reissig, H.; Wiehe, A. *J. Org. Chem.* **2015**, *80*, 5133−5143. (c) Palao, E.; de la Moya, S.; Agarrabeitia, A. R.; Esnal, I.; Bañuelos, J.; López -Arbeloa, A.; Ortiz, M. J. *Org. Lett.* **2014**, *16*, 4364−4367. (d) Yokoi, H.; Hiroto, S.; Shinokubo, H. *Org. Lett.* **2014**, *16*, 3004. (e) Ulrich, G.; Ziessel, R.; Haefele, A. *J. Org. Chem.* **2012**, *77*, 4298−4311. (f) Ulrich, G.; Haefele, A.; Retailleau, P.; Ziessel, R. *J. Org. Chem.* **2012**, *77*, 5036−5048. (g) Lakshmi, V.; Ravikanth, M. *J. Org. Chem.* **2011**, *76*, 8466−8471.

(5) (a) Thorat, K. G.; Kamble, P.; Mallah, R.; Ray, A. K.; Sekar, N. *J. Org. Chem.* **2015**, *80*, 6152−6164. (b) Gutierrez-Ramos, B. D.; Banuelos, J.; Arbeloa, T.; Arbeloa, I. L.; Gonzalez-Navarro, P. E.; Wrobel, K.; Cerdan, L.; Garcia-Moreno, I.; Costela, A.; Peña-Cabrera, E. *Chem. - Eur. J.* **2015**, *21*, 1755−1764. (c) Gómez-Durán, C. FA; Esnal, I.; Valois-Escamilla, I.; Urías-Benavides, A.; Bañuelos, J.; Arbeloa, I. L.; García-Moreno, I.; Peña-Cabrera, E. *Chem. - Eur. J.* **2016**, *22*, 1048−1061.

(6) (a) Zhang, X.; Xiao, Y.; Qi, J.; Qu, J.; Kim, B.; Yue, X.; Belfield, K. D. *J. Org. Chem.* **2013**, *78*, 9153−9160. (b) Wang, D.; Fan, J.; Gao, X.; Wang, B.; Sun, S.; Peng, X. *J. Org. Chem.* **2009**, *74*, 7675−7683. (c) Ehrenschwender, T.; Wagenknecht, H.-A. *J. Org. Chem.* **2011**, *76*, 2301−2304. (d) Kim, J.-Y.; Sahu, S.; Yau, Y.-H.; Wang, X.; Shochat, S. G.; Nielsen; Per, H.; Dueholm, M. S.; Otzen, D. E.; Lee, J.; Santos, M. M. S. D.; Yam, J. K. H.; Kang, N.-Y.; Park, S.-J.; Kwon, H.; Seviour, T.; Yang, L.; Givskov, M.; Chang, Y.-T. *J. Am. Chem. Soc.* **2016**, *138*, 402−407.

(7) (a) Yuan, L.; Lin, W.; Zheng, K.; He, L.; Huang, W. *Chem. Soc. Rev.* **2013**, *42*, 622−661. (b) Ekmekci, Z.; Yilmaz, M. D.; Akkaya, E. U. *Org. Lett.* **2008**, *10*, 461−464. (c) Atilgan, S.; Ozdemir, T.; Akkaya, E. U. *Org. Lett.* **2008**, *10*, 4065−4067. (d) Chen, Y.; Wang, H.; Wan, L.; Bian, Y.; Jiang, J. *J. Org. Chem.* **2011**, *76*, 3774−3781. (e) Wang, F.; Zhu, Y.; Zhou, L.; Pan, L.; Cui, Z.; Fei, Q.; Luo, S.; Pan, D.; Huang, Q.; Wang, R.; Zhao, C.; Tian, H.; Fan, C. *Angew. Chem., Int. Ed.* **2015**, *54*, 7349−7353.

(8) (a) Golovkova, T. A.; Kozlov, D. V.; Neckers, D. C. *J. Org. Chem.* **2005**, *70*, 5545−5549. (b) Tomasulo, M.; Deniz, E.; Alvarado, R. J.; Raymo, F. M. *J. Phys. Chem. C* **2008**, *112*, 8038−8045. (c) Moreno, J.; Schweighöfer, F.; Wachtveitl, J.; Hecht, S. *Chem. - Eur. J.* **2016**, *22*, 1070−1075.

(9) (a) Bura, T.; Leclerc, N.; Fall, S.; Lévêque, P.; Heiser, T.; Retailleau, P.; Rihn, S.; Mirloup, A.; Ziessel, R. *J. Am. Chem. Soc.* **2012**, *134*, 17404−17407. (b) Chen, J. J.; Conron, S. M.; Erwin, P.; Dimitriou, M.;

McAlahney, K.; Thompson, M. E. *ACS Appl. Mater. Interfaces* **2015**, *7*, 662−669.

(10) (a) Zhao, J.; Wu, W.; Sun, J.; Guo, S. *Chem. Soc. Rev.* **2013**, *42*, 5323−5351. (b) Huang, L.; Yang, W.; Zhao, J. *J. Org. Chem.* **2014**, *79*, 10240−10255. (c) Ji, S.; Ge, J.; Escudero, D.; Wang, Z.; Zhao, J.; Jacquemin, D. *J. Org. Chem.* **2015**, *80*, 5958−5963. (d) Turan, I. S.; Yildiz, D.; Turksoy, A.; Gunaydin, G.; Akkaya, E. U. *Angew. Chem., Int. Ed.* **2016**, *55*, 2875−2878. (e) Awuah, S. G.; You, Y. *RSC Adv.* **2012**, *2*, 11169−11183.

(11) (a) Awuah, S. G.; Polreis, J.; Biradar, V.; You, Y. *Org. Lett.* **2011**, *13*, 3884−3887. (b) Uppal, T.; Hu, X.; Fronczek, F. R.; Maschek, S.; Bobadova-Parvanova, P.; Vicente, M. G. *Chem. - Eur. J.* **2012**, *18*, 3893−3905. (c) Yang, Y.; Guo, Q.; Chen, H.; Zhou, Z.; Guo, Z.; Shen, Z. *Chem. Commun.* **2013**, *49*, 3940−3942. (d) Awuah, S. G.; Das, S. K.; D'Souza, F.; You, Y. *Chem. - Asian J.* **2013**, *8*, 3123−3132. (e) Yamazawa, S.; Nakashima, M.; Suda, Y.; Nishiyabu, R.; Kubo, Y. *J. Org. Chem.* **2016**, *81*, 1310−1315. (f) Sun, Z.-B.; Guo, M.; Zhao, C.-H. *J. Org. Chem.* **2016**, *81*, 229−237.

(12) (a) Ni, Y.; Lee, S.; Son, M.; Aratani, N.; Ishida, M.; Samanta, A.; Yamada, H.; Chang, Y.-T.; Furuta, H.; Kim, D.; Wu, J. *Angew. Chem., Int. Ed.* **2016**, *55*, 2815−2819. (b) Jiao, C.; Zhu, L.; Wu, J. *Chem. - Eur. J.* **2011**, *17*, 6610−6614. (c) Yu, C.; Jiao, L.; Li, T.; Wu, Q.; Miao, W.; Wang, J.; Wei, Y.; Mu, X.; Hao, E. *Chem. Commun.* **2015**, *51*, 16852−16855. (d) Wang, J.; Wu, Q.; Wang, S.; Yu, C.; Li, J.; Hao, E.; Wei, Y.; Mu, X.; Jiao, L. *Org. Lett.* **2015**, *17*, 5360−5363.

(13) (a) Lu, H.; Mack, J.; Yang, Y.; Shen, Z. *Chem. Soc. Rev.* **2014**, *43*, 4778−4823. (b) Ni, Y.; Wu, J. *Org. Biomol. Chem.* **2014**, *12*, 3774−3791. (c) Boens, N.; Verbelen, B.; Dehaen, W. *Eur. J. Org. Chem.* **2015**, *2015*, 6577−6595. (d) Lakshmi, V.; Rao, M. R.; Ravikanth, M. *Org. Biomol. Chem.* **2015**, *13*, 2501−2517.

(14) (a) Leen, V.; Yuan, P.; Wang, L.; Boens, N.; Dehaen, W. *Org. Lett.* **2012**, *14*, 6150−6153. (b) Lakshmi, V.; Ravikanth, M. *J. Org. Chem.* **2013**, *78*, 4993−5000. (c) Duran Sampedro, G.; Palao, E.; Agarrabeitia, A. R.; de la Moya, S.; Boens, N.; Ortiz, M. J. *RSC Adv.* **2014**, *4*, 19210−19213. (d) Wang, J.; Wu, Q.; Wang, S.; Yu, C.; Li, J.; Hao, E.; Wei, Y.; Mu, X.; Jiao, L. *Org. Lett.* **2015**, *17*, 5360−5363.

(15) (a) Wang, H.; Fronczek, F. R.; Vicente, M. G. H.; Smith, K. M. *J. Org. Chem.* **2014**, *79*, 10342−10352. (b) Wang, H.; Vicente, M. G.; Fronczek, F. R.; Smith, K. M. *Chem. - Eur. J.* **2014**, *20*, 5064−5074. (c) Zhao, N.; Xuan, S.; Fronczek, F. R.; Smith, K. M.; Vicente, M. G. H. *J. Org. Chem.* **2015**, *80*, 8377−8383. (d) Zhao, N.; Vicente, M. G.; Fronczek, F. R.; Smith, K. M. *Chem. - Eur. J.* **2015**, *21*, 6181−6192. (e) Jiao, L.; Yu, C.; Liu, M.; Wu, Y.; Cong, K.; Meng, T.; Wang, Y.; Hao, E. *J. Org. Chem.* **2010**, *75*, 6035−6038. (f) Jiao, L.; Yu, C.; Uppal, T.; Liu, M.; Li, Y.; Zhou, Y.; Hao, E.; Hu, X.; Vicente, M. G. H. *Org. Biomol. Chem.* **2010**, *8*, 2517−2519.

(16) (a) Verbelen, B.; Boodts, S.; Hofkens, J.; Boens, N.; Dehaen, W. *Angew. Chem., Int. Ed.* **2015**, *54*, 4612−4616. (b) Verbelen, B.; Rezende, L. C. D.; Boodts, S.; Jacobs, J.; Van Meervelt, L.; Hofkens, J.; Dehaen, W. *Chem. - Eur. J.* **2015**, *21*, 12667−12675. (c) Verbelen, B.; Verbelen, B.; Leen, V.; Wang, L.; Boens, N.; Dehaen, W. *Chem. Commun.* **2012**, *48*, 9129−9131.

(17) (a) Buyukcakir, O.; Bozdemir, O. A.; Kolemen, S.; Erbas, S.; Akkaya, E. U. *Org. Lett.* **2009**, *11*, 4644−4647. (b) Bura, T.; Retailleau, P.; Ulrich, G.; Ziessel, R. *J. Org. Chem.* **2011**, *76*, 1109−1117. (c) Shivran, N.; Mula, S.; Ghanty, T. K.; Chattopadhyay, S. *Org. Lett.* **2011**, *13*, 5870−5873. (d) Palao, E.; Agarrabeitia, A. R.; Bañuelos-Prieto, J.; Lopez, T. A.; Lopez-Arbeloa, I.; Armesto, D.; Ortiz, M. J. *Org. Lett.* **2013**, *15*, 4454−4457.

(18) (a) Haugland, R. P. *The handbook: a guide to fluorescent probes and labeling technologies*; Invitrogen Corporation: USA, 2005. (b) Dale, C. L.; Hill, S. J.; Kellam, B. *Med. Chem. Commun.* **2012**, *3*, 333−338. (c) Mizusawa, K.; Takaoka, Y.; Hamachi, I. *J. Am. Chem. Soc.* **2012**, *134*, 13386−13395. (d) Baker, J. G.; Adams, L. A.; Salchow, K.; Mistry, S. N.; Middleton, R. J.; Hill, S. J.; Kellam, B. *J. Med. Chem.* **2011**, *54*, 6874−6887.

(19) (a) Haugland, R. P.; Kang, H. C. U. S. Patent 5248782, 1993. (b) Rao, M. R.; Tiwari, M. D.; Bellare, J. R.; Ravikanth, M. *J. Org. Chem.* **2011**, *76*, 7263−7268. (c) Lakshmi, V.; Lee, W.-Z.; Ravikanth, M.

Dalton Trans. **2014**, *43*, 16006−16014. (d) Zhang, M.; Hao, E.; Xu, Y.; Zhang, S.; Zhu, H.; Wang, Q.; Yu, C.; Jiao, L. *RSC Adv.* **2012**, *2*, 11215−11218. (e) Kaur, T.; Lakshmi, V.; Ravikanth, M. *RSC Adv.* **2013**, *3*, 2736−2745.

(20) Yu, C.; Xu, Y.; Jiao, L.; Zhou, J.; Wang, Z.; Hao, E. *Chem. - Eur. J.* **2012**, *18*, 6437−6442.

(21) Alberto, M. E.; Simone, B. C.; De Mazzone, G.; Quartarolo, A. D.; Russo, N. *J. Chem. Theory Comput.* **2014**, *10*, 4006−4013.

(22) Yu, C.; Jiao, L.; Zhang, P.; Feng, Z.; Cheng, C.; Wei, Y.; Mu, X.; Hao, E. *Org. Lett.* **2014**, *16*, 3048−3051.

(23) (a) Wang, D.; Fan, J.; Gao, X.; Wang, B.; Sun, S.; Peng, X. *J. Org. Chem.* **2009**, *74*, 7675−7683. (b) Jiao, L.; Pang, W.; Zhou, J.; Wei, Y.; Mu, X.; Hao, E. *J. Org. Chem.* **2011**, *76*, 9988−9996.

(24) (a) Schmitt, A.; Hinkeldey, B.; Wild, M.; Jung, G. *J. Fluoresc.* **2009**, *19*, 755−758. (b) Arroyo, I. J.; Hu, R.; Merino, G.; Tang, B. Z.; Peña-Cabrera, E. *J. Org. Chem.* **2009**, *74*, 5719−5722.

(25) Arroyo, I. J.; Hu, R.; Tang, B. Z.; Lopez, F. I.; Pena-Cabrera, E. *Tetrahedron* **2011**, *67*, 7244−7250.

(26) (a) Sunahara, H.; Urano, Y.; Kojima, H.; Nagano, T. *J. Am. Chem. Soc.* **2007**, *129*, 5597−5604. (b) Granzhan, A.; Ihmels, H.; Viola, G. *J. Am. Chem. Soc.* **2007**, *129*, 1254−1267. (c) Jiang, T.; Zhang, P.; Yu, C.; Yin, J.; Jiao, L.; Dai, E.; Wang, J.; Wei, Y.; Mu, X.; Hao, E. *Org. Lett.* **2014**, *16*, 1952−1955.

(27) Rurack, K.; Kollmannsberger, M.; Daub, J. *Angew. Chem., Int. Ed.* **2001**, *40*, 385−387.

(28) (a) Tang, B.; Liu, X.; Xu, K.; Huang, H.; Yang, G.; An, L. *Chem. Commun.* **2007**, 3726−3728. (b) Thivierge, C.; Han, R.; Jenkins, M.; Burgess, K. *J. Org. Chem.* **2011**, *76*, 5219−5228. (c) Chen, Y.; Qi, D.; Zhao, L.; Cao, W.; Huang, C.; Jiang, J. *Chem. - Eur. J.* **2013**, *19*, 7342−7347. (d) Jiang, X.-D.; Su, Y.; Yue, S.; Li, C.; Yu, H.; Zhang, H.; Sun, C.-L.; Xiao, L.-J. *RSC Adv.* **2015**, *5*, 16735−16739.

(29) Momeni, M. R.; Brown, A. *J. Chem. Theory Comput.* **2015**, *11*, 2619−2632.

(30) Diana, P.; Martorana, A.; Barraja, P.; Montalbano, A.; Carbone, A.; Cirrincione, G. *Tetrahedron* **2011**, *67*, 2072−2080.

(31) Magde, D.; Brannon, J. H.; Cremers, T. L.; Olmsted, J. *J. Phys. Chem.* **1979**, *83*, 696−699.

(32) Killoran, J.; Allen, L.; Gallagher, J. F.; Gallagher, W. M.; O'Shea, D. F. *Chem. Commun.* **2002**, 1862−1863.

(33) Lakowicz, J. R. *Principles of Fluorescence Spectroscopy*; Springer: New York, 2006.

(34) Sheldrick, G. M. *SADABS*, Program for Empirical Absorption Correction of Area Detector Data; University of Göttingen: Germany, 1996.

(35) Sheldrick, G. M. *SHELXTL 5.10* for Windows NT: Structure Determination Software Programs; Bruker Analytical X-ray Systems, Inc.: Madison, WI, 1997.

(36) Frisch, M. J.; Trucks, G. W. et al. *Gaussian 09*, revision D.01, Gaussian, Inc.: Wallingford, CT, 2010.